Human Molecular Genetics, 2008, Vol. 17, No. 18 **2753–2765**
doi:10.1093/hmg/ddn160
Advance Access published on May 27, 2008

Beyond the sarcomere: CSRP3 mutations cause hypertrophic cardiomyopathy

Christian Geier[1,2,*,†], Katja Gehmlich[3,†], Elisabeth Ehler[4], Sabine Hassfeld[1], Andreas Perrot[2], Katrin Hayess[5], Nuno Cardim[6], Katrin Wenzel[2], Bettina Erdmann[7], Florian Krackhardt[1], Maximilian G. Posch[2], Angelika Bublak[8], Herbert Nägele[9], Thomas Scheffold[10], Rainer Dietz[1,2], Kenneth R. Chien[11], Simone Spuler[12], Dieter O. Fürst[13], Peter Nürnberg[14] and Cemil Özcelik[1,2]

[1]Charité Universitätsmedizin Berlin, Campus Virchow-Klinikum, Med. Klinik m. S. Kardiologie, 13353 Berlin, Germany, [2]Experimental and Clinical Research Center (ECRC) at the Max Delbrück Center for Molecular Medicine (MDC), Cardiovascular Genetics, 13125 Berlin, Germany, [3]Department of Medicine, University College London, London WC1E 6DD, UK, [4]The Randall Division of Cell and Molecular Biophysics and the Cardiovascular Division, King's College London, London SE1 1UL, UK, [5]Bundesinstitut für Risikobewertung – ZEBET, 12277 Berlin, Germany, [6]Faculdada de Ciências Médicas da Universidade Nova de Lisboa, 1700-093 Lisbon, Portugal, [7]Max-Delbrück-Centrum für Molekulare Medizin (MDC) Berlin-Buch, 13125 Berlin, Germany, [8]DRK Kliniken Berlin Köpenick, Medizinische Klinik I, 12559 Berlin, Germany, [9]Krankenhaus Reinbek, St Adolfstift, Medizinische Klinik, 21465 Hamburg-Reinbek, Germany, [10]Institut für Herz-Kreislaufforschung an der Universität Witten/Herdecke, 44225 Dortmund, Germany, [11]Cardiovascular Research Centre, Massachusetts General Hospital, Department of Cell Biology, Harvard Medical School, Harvard Stem Cell Institute, Boston, MA 02114, USA, [12]Charité Universitätsmedizin Berlin, Experimental and Clinical Research Centre (ECRC), Muscle Research Unit, 13125 Berlin, Germany, [13]Abteilung Molekulare Zellbiologie, Institut für Zellbiologie, Universität Bonn, 53121 Bonn, Germany and [14]Cologne Centre for Genomics and Institute for Genetics, University of Cologne, 50674 Köln, Germany

Received March 12, 2008; Revised May 1, 2008; Accepted May 21, 2008

Hypertrophic cardiomyopathy (HCM) is a frequent genetic cardiac disease and the most common cause of sudden cardiac death in young individuals. Most of the currently known HCM disease genes encode sarcomeric proteins. Previous studies have shown an association between *CSRP3* missense mutations and either dilated cardiomyopathy (DCM) or HCM, but all these studies were unable to provide comprehensive genetic evidence for a causative role of *CSRP3* mutations. We used linkage analysis and identified a *CSRP3* missense mutation in a large German family affected by HCM. We confirmed *CSRP3* as an HCM disease gene. Furthermore, *CSRP3* missense mutations segregating with HCM were identified in four other families. We used a newly designed monoclonal antibody to show that muscle LIM protein (MLP), the protein encoded by *CSRP3*, is mainly a cytosolic component of cardiomyocytes and not tightly anchored to sarcomeric structures. Our functional data from both *in vitro* and *in vivo* analyses suggest that at least one of MLP's mutated forms seems to be destabilized in the heart of HCM patients harbouring a *CSRP3* missense mutation. We also present evidence for mild skeletal muscle disease in affected persons. Our results support the view that HCM is not exclusively a sarcomeric disease and also suggest that impaired mechano-sensory stress signalling might be involved in the pathogenesis of HCM.

*To whom correspondence should be addressed at: Charité Universitätsmedizin Berlin, Med. Klinik m. S. Kardiologie, Augustenburger Platz 1, 13353 Berlin, Germany. Tel: +49 30450553055; Fax: +49 30450565955; Email: christian.geier@charite.de
†Each of these authors contributed equally to this manuscript.

INTRODUCTION

Hypertrophic cardiomyopathy [HCM (OMIM CMH, http://www.ncbi.nlm.nih.gov/entrez/dispomim.cgi?id=192600)] is the most common genetic myocardial disease with a 0.2% prevalence in adults (1) and is the most frequent cause of sudden cardiac death in young persons (2). Left ventricular hypertrophy in the absence of other causes is the clinical hallmark. In the myocardium, areas of myocyte disarray are typically found, an uncommon situation in other forms of cardiac hypertrophy (3). Over 450 mutations in at least 11 genes encoding sarcomeric proteins have been reported with an autosomal-dominant mode of inheritance, suggesting that HCM is a sarcomeric disease (4,5). However, systematic mutation screening in genes encoding sarcomeric proteins resolves only about two-thirds of patients (6,7). Thus, unrecognized genes are likely. Muscle LIM protein (MLP, also known as cysteine and glycine-rich protein 3, CRP3) is a muscle-specific LIM-only protein. MLP has been described as a cytoskeletal protein (8), but has also been associated with sarcomeric structures (9). The previously used polyclonal antisera might explain this discrepancy. MLP was suggested to act in concert with titin and telethonin as a stretch sensor (10). Mice with a functional knockout of MLP develop either massive myocardial hypertrophy leading to rapid congestive heart failure or a phenotype resembling dilated cardiomyopathy (DCM) in humans (9). Mutations in *CSRP3*, the human gene coding for MLP, have been associated with either DCM or HCM in humans (10,11). However, a causative relationship could not be proven in either of these studies because the families were too small to allow conclusive genomic linkage analysis.

We show additional evidence that *CSRP3* mutations cause HCM. We found that a previously described *CSRP3* p.W4R variant is not sufficient to cause DCM. We demonstrate that the *CSRP3* gene product is predominantly cytosolic, rather than confined to sarcomeric structures. Even though this challenges the proposed function of MLP as a stretch sensor itself, MLP seems to have crucial functions in the downstream signal transduction in response to mechanical stress (10). We suggest that HCM could involve improper response to myocardial stress sensing.

RESULTS

Genealogy was performed in a German family where our previous mutation screening had revealed a heterozygous *CSRP3* c.172T>G missense mutation, but no mutation in any known sarcomeric HCM disease gene in the three affected patients (11). The core family was too small for conclusive linkage analysis. We were able to track and examine another 51 living relatives (see Supplementary Material, Fig. S1). Five fulfilled the diagnostic criteria of HCM. Linkage analysis was performed in the extended family. Microsatellite analysis adjacent to the loci of all known HCM disease genes resulted in the exclusion of linkage to any of these loci with logarithm of odds (LOD) scores ≤ 2 (Supplementary Material, Table S1). Genome-wide linkage and haplotype analyses for chromosome 11 markers in this kindred (family H1, Fig. 1A and B) revealed a genomic interval of 5.5 cM between D11S1981 and D11S1755 as the only linkage support interval. The maximum multipoint LOD score was as high as 5.9 at $\theta = 0$, assuming a reduced penetrance of 0.9. The critical interval comprised the genomic locus of *CSRP3* with chromosomal localization 11p15.1 matching the previously mapped locus on chromosome 11 (12). We also included two additional families (Supplementary Material, Fig. S2) with previously described (11) heterozygous *CSRP3* mutations [c.131T>C corresponding to p.L44P in family H2 and compound mutation (c.160T>A; c.161C>G; c.164A>G) predicting p.(S54R; E55G) in family H3] into haplotype analysis and found segregation of the phenotype with markers at the *CSRP3* locus.

We next analyzed 652 DCM and 354 HCM patients by direct sequencing of *CSRP3* exons 2 and 3, the regions with known cardiomyopathy-associated variants (10,11). Five hundred and thirty-three phenotypically normal probands served as controls. By sequencing exon 3, we identified two additional HCM patients harbouring the heterozygous missense mutation c.136A>C that predicts the exchange of the highly conserved serine in codon 46 to arginine (p.S46R). Kindred segregation analysis of these two patients (families H4 and H5, Fig. 1C) demonstrated cosegregation in family H5 and the absence of the mutation in the unaffected son of the patient in family H4. Although the two families were unrelated, they may nevertheless share a common ancestor, since index patient haplotype analysis of both families revealed an identical haplotype based on three markers (D11S2368, D11S5038, D11S5039) adjoining the *CSRP3* locus. None of the four different *CSRP3* exon 3 mutations was found in the control group. Furthermore, no coding mutations within exon 3 were found in the DCM patients.

Clinical characteristics of the five families H1–H5 were typical for HCM (see Supplementary Material, Table S2). Most affected persons had pronounced hypertrophy and reported an onset of symptoms in young adulthood. A family history of sudden cardiac death was present in two families (H1 and H3). Cardiac magnetic resonance images were available for one individual (H3-II:1) and demonstrated regional late gadolinium enhancement representing myocardial fibrosis and scarring. Extent and localization of left ventricular hypertrophy in the patients harbouring *CSRP3* exon 3 mutations showed remarkable inter-individual variability. While most individuals with marked hypertrophy had asymmetrical septal hypertrophy, we also found one affected relative with severe apical hypertrophy (H1-IV:7), one patient (H3-II:1) with concentric and another one (H2-III:1) with mid-ventricular hypertrophy (clinical data documented in Supplementary Material, Table S2).

By sequencing *CSRP3* exon 2, the previously described p.W4R variant (10) was identified in seven individuals. Interestingly, three (0.5%) were DCM patients, two (0.6%) HCM patients and two (0.4%) were controls. The respective DCM kindreds D1, D2, D3 and HCM kindreds H6 and H7 are shown in Supplementary Material, Figure S3 and clinical data are summarized in Supplementary Material, Tables S2 and S3. Segregation analysis in the cardiomyopathy patient families with the p.W4R variant resulted in exclusion of segregation in HCM family H6. Cosegregation in families D1, D2, D3 and H7 was doubtful because the cosegregation assumption would require us to presuppose an implausibly low penetrance. Instead, a known *MYBPC3* nonsense-mutation

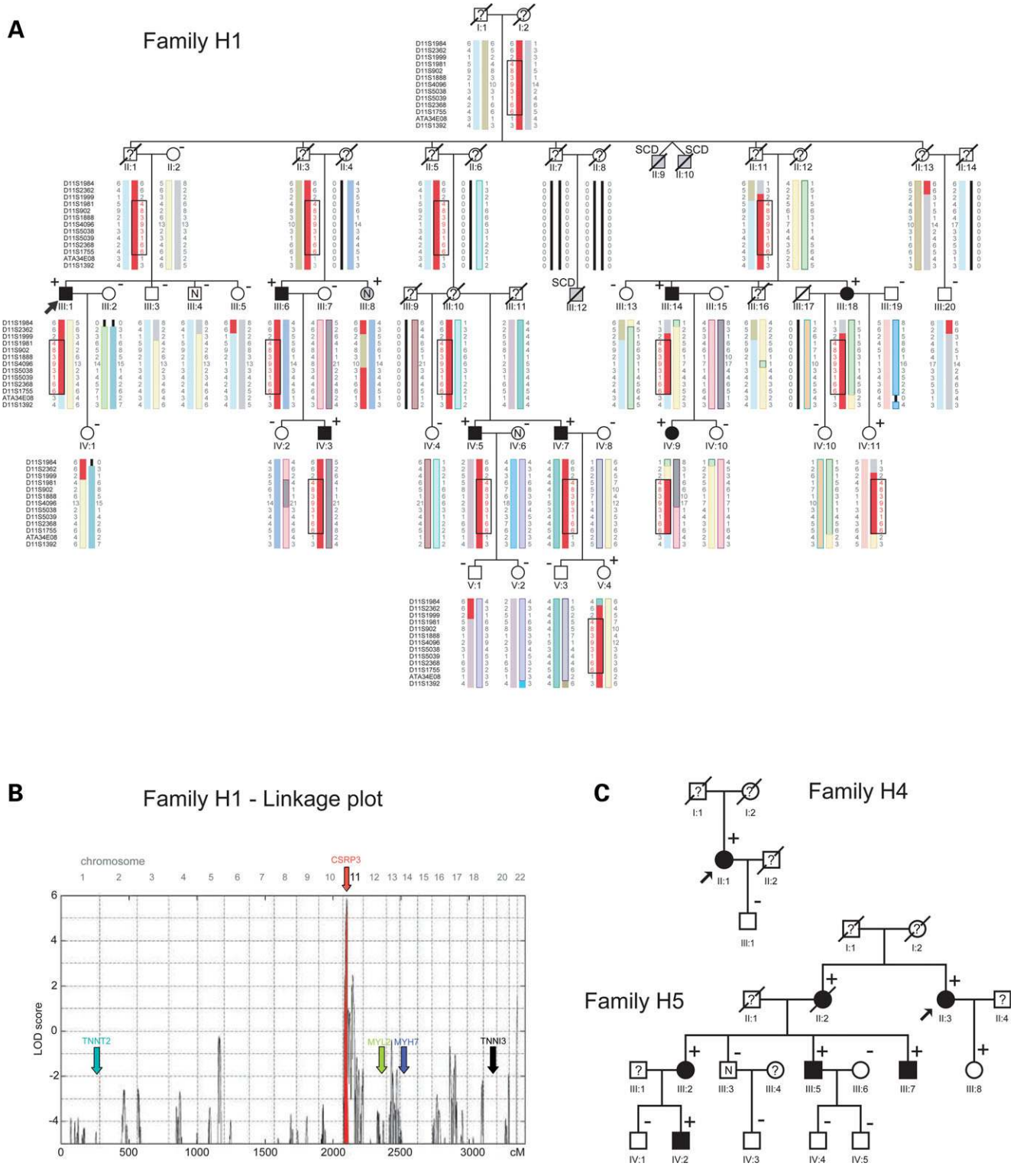

Figure 1. Genetic evidence for *CSRP3* as an HCM disease gene. (**A**) Pedigree including the results of haplotype analysis of HCM family H1. Squares, males; circles, females. Open symbols represent unaffected subjects; solid symbols represent individuals suffering from HCM and slanted bars represent deceased individuals. Question marks denote individuals with unknown disease status, capital 'N' denotes individuals not classifiable with respect to affected status, the black arrow indicates the index patient. SCD marks individuals who suffered sudden cardiac death. Grey symbols mark probably affected individuals. Plus symbols mark the presence of a heterozygous *CSRP3* c.172T>G missense mutation. The microsatellite alleles contributing to the haplotype of all affecteds are marked in red. (**B**) Results of multipoint linkage mapping in family H1. Maximal LOD scores are plotted against relative genomic distances. The area under the maximum peak is filled in red. The genomic position of the *CSRP3* locus is indicated by the red arrow. For clarity, only colored arrows highlight a few positions of the other known HCM gene loci. (**C** and **D**) Pedigrees of HCM families H4 and H5. Plus symbols mark the presence of heterozygous *CSRP3* c.136A>C missense mutation. Other symbols are as described in (A).

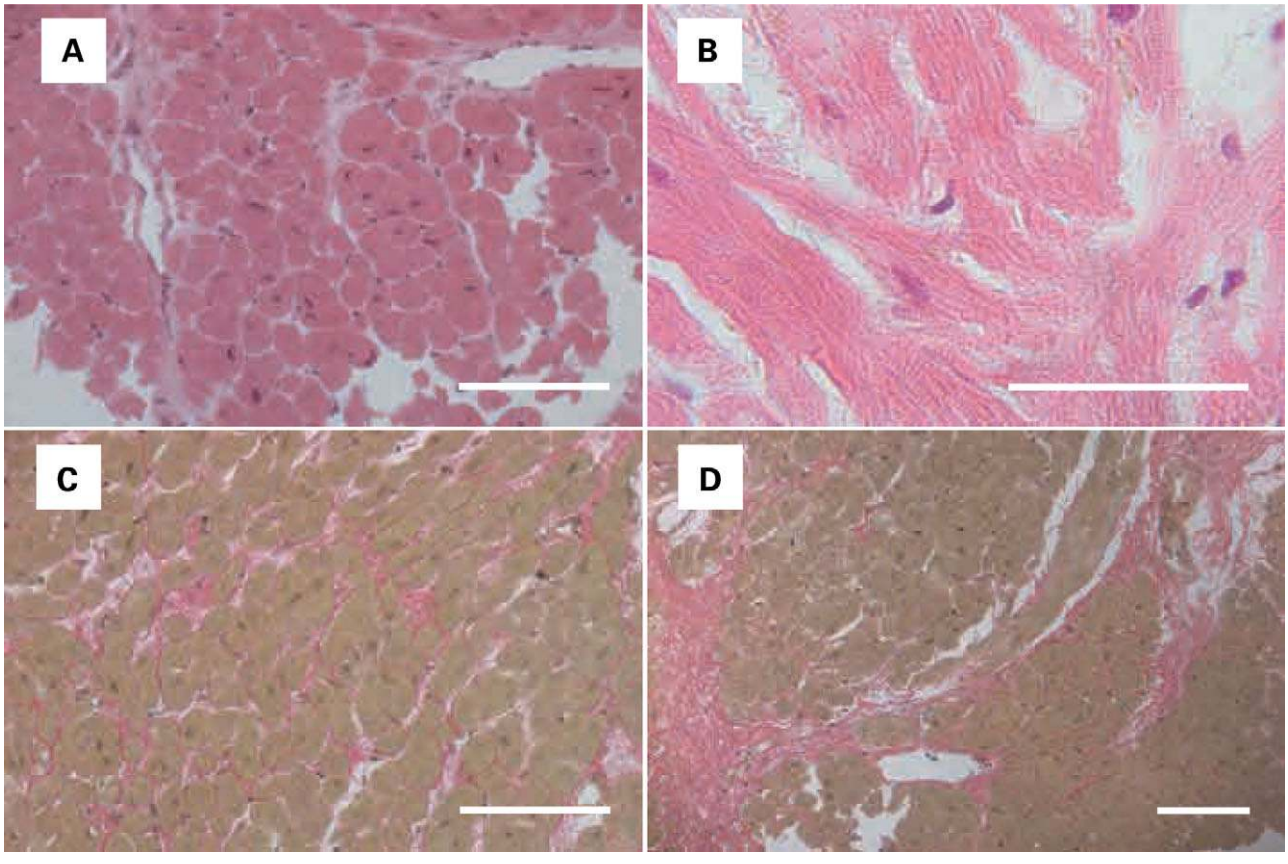

Figure 2. Ultrastructural phenotype of HCM caused by MLP p.C58G mutant demonstrating the typical ultrastructural changes of HCM. Myocardial histology of myectomy material of the index patient of family H1 harbouring heterozygous MLP p.C58G mutation (**A, C** and **D**). (A) Hematoxylin-eosin stained section demonstrating variably hypertrophied cardiomyocytes. (**B**) Hematoxylin-eosin stained section of a myocardial biopsy (posterolateral left ventricular wall) of the same patient showing myocyte disarray. (C and D) Picrosirius red stained sections highlight collagen in pink color. It demonstrates increased interstitial and perivascular fibrosis and areas of scarring (D). Scale bars represent 100 μm (A–D).

(13) was identified as the causative mutation in family H6 (Supplementary Material, Table S2). In the HCM families, no correlation was observed between the severity of the disease and/or progression to heart failure and the occurrence of the p.W4R variant. Both controls (aged 61 and 75 years) harbouring the MLP p.W4R variant had a negative family history of heart failure. Hence, we conclude that, in contrast to the mutations found in exon 3 of *CSRP3*, the p.W4R variant is not sufficient to cause cardiomyopathy.

To investigate potential structural changes induced by a disease-causing MLP mutation, we analyzed myocardial biopsies of the family H1 index patient (H1-III:1). The biopsies demonstrated histological patterns typical for HCM caused by sarcomeric protein gene mutations, namely variably hypertrophied cardiomyocytes, myocyte disarray, perivascular and interstitial fibrosis and scarring (Fig. 2). Electron microscopy also displayed typical nuclear pleomorphism with bizarre lobulated cardiomyocyte nuclei, another common feature of HCM, while sarcomeric ultrastructure showed no gross abnormalities (Supplementary Material, Fig. S4).

Since previous localization and protein-binding studies with MLP have yielded conflicting results, we raised a murine monoclonal antibody (mAB 79D2) specific for MLP. We performed extensive tests to prove the specificity of this antibody and used it in western blotting, immunoprecipitation and immunofluorescence experiments (Figs 3 and 4). Surprisingly, immunofluorescence microscopy of cardiac tissue using this monoclonal antibody (Figs 3F and 4A) revealed general cytoplasmic staining with no or very little preference for Z-band structures. Furthermore, staining of isolated neonatal rat cardiomyocytes (NRCs) showed diffuse cytoplasmic MLP localization (Fig. 3D, see also Fig. 4C), which was absent in myocardial fibroblasts (Fig. 3D). In myocardial extracts, MLP was already extracted quantitatively under low-salt conditions using a Triton X-100 buffer (Fig. 4B). This fraction contained essentially only cytosolic proteins, whereas sarcomeric proteins of both Z-disk and M-band were not extractable under this condition (Fig. 4B). Likewise, treatment of NRCs with Triton X-100 prior to fixation resulted in a complete MLP washout, whereas sarcomeric structures were preserved (Fig. 4C). Thus, MLP was more readily extracted than all myofibrillar proteins, suggesting that MLP is mainly a cytosolic component of cardiomyocytes that is neither solely sarcomeric nor tightly associated with sarcomeric structures.

To assess the consequences of disease-causing MLP mutations on MLP localization, rat neonatal cardiomyocytes were transfected with human *CSRP3* cDNA (wild-type versus mutants). These experiments also indicated a diffuse

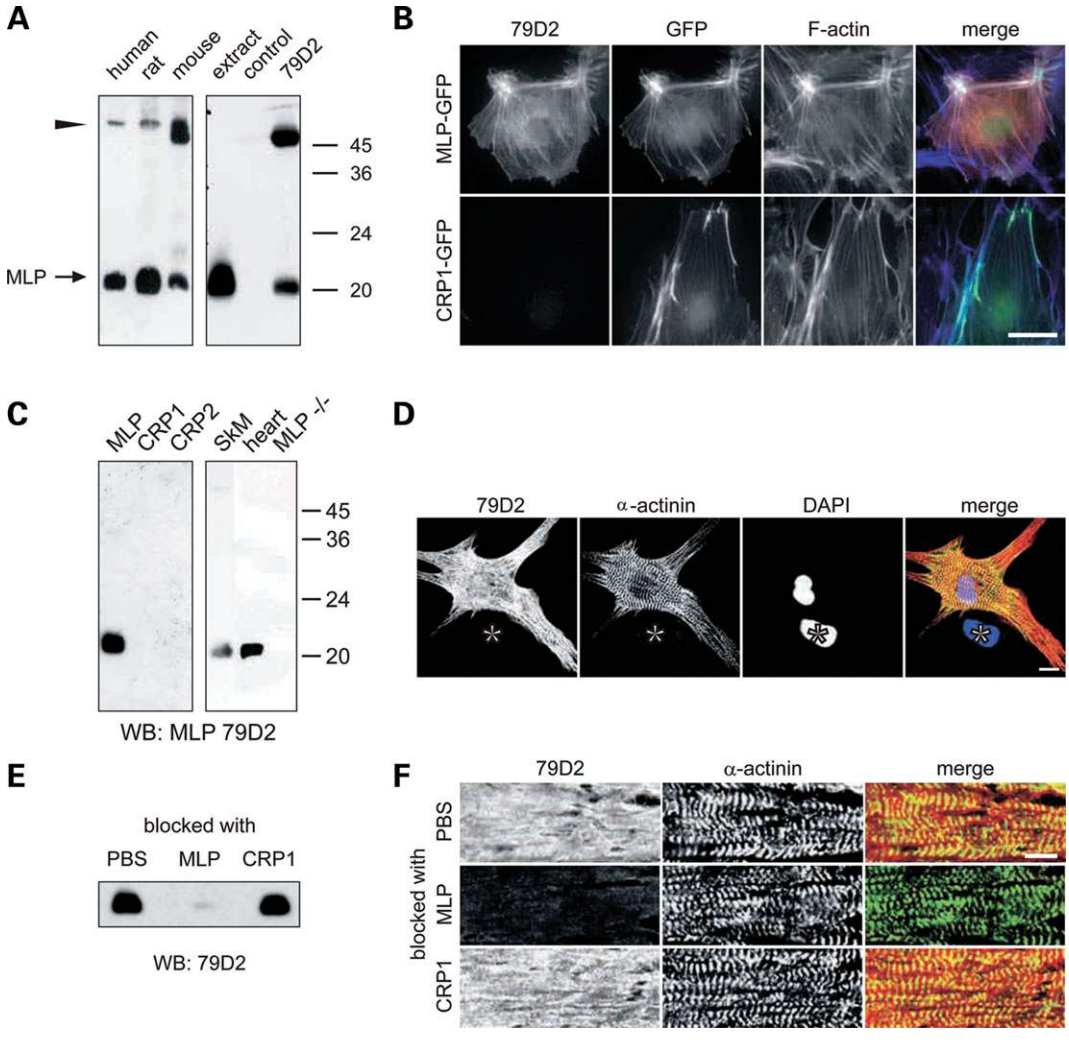

Figure 3. Characterization of mAB 79D2: (**A**) Left: mAB 79D2 recognizes endogenous MLP protein (arrow) in cardiac tissue extracts of different species. An occasionally observed, slower migrating band (arrowhead) corresponds to a cross-reaction of the secondary antibody with immunoglobulins. Right: endogenous MLP was immunoprecipitated by mAB 79D2 from cardiac tissue protein extracts (third lane), but not in control immunoprecipitation without antibody (second lane). The extract used for the experiment is shown in the first lane. (**B**) mAB 79D2 specifically recognizes MLP in immunofluorescence experiments: PtK2 cells, which lack endogenous MLP, were transfected with MLP–GFP (upper row) or CRP1–GFP fusion protein (lower row). Cells were stained for MLP with mAB 79D2 (first lane), for comparison the GFP signal is given (second lane). F-actin was visualized with phalloidin (third lane) and pictures are merged on the right (79D2, red; GFP, green; F-actin, blue). Scale bar is 25 μm. (**C**) The mAB 79D2 specifically reacted with bacterially expressed recombinant MLP and showed no cross-reaction with CRP1 or CRP2 in western blot experiments. In human tissues, endogenous protein was detected as a band of expected size (predicted 20.8 kDa) in skeletal muscle (SkM) and cardiac tissue (heart). The absence of a signal in cardiac tissue of $MLP^{-/-}$ mice confirmed the specificity of the antibody. (**D**) mAB 79D2 specifically recognises MLP in cardiomyocytes, but is negative on myocardial fibroblasts: co-cultures of neonatal cardiomyocytes and myocardial fibroblasts were stained with mAB 79D2 (first column). Cardiomyocytes were identified by Z-discs stain of α-actinin 2 (second column). DAPI (third column) was used to visualize nuclei in both cell types. Myocardial fibroblasts (asterisks) were identified by the absence of α-actinin 2 stain and by their nuclear morphology (single-nucleated cells with larger nuclei than cardiomyocytes). Merged pictures: MLP red, α-actinin 2, green, DAPI blue; scale bar is 10 μm. Note the absence of a signal with mAB 79D2 in myocardial fibroblasts. (**E** and **F**) Antigen-blocking assay: pre-saturation of mAB 79D2 with recombinant MLP protein, but not with recombinant CRP1 protein abolished signals in Western blotting (E) and immunofluorescence (F) of cardiac tissue samples. Un-saturated mAB 79D2 served as a control (PBS). For comparison, Z-discs were visualized by staining for α-actinin (middle); merged picture: MLP, red; α-actinin, green; scale bar is 10 μm. Note that mAB 79D2 was specifically blocked by MLP, but not by control protein.

cytoplasmic localization of MLP, but they failed to indicate any significant differences between wild-type and mutant proteins at this level (Fig. 5E). However, immunohistochemistry of a myocardial biopsy sample from the index patient of family H1 revealed areas of inhomogeneous and patchy MLP staining (Supplementary Material, Fig. S5). In contrast to these relatively minor alterations in MLP localization, western blot analysis showed a dramatic reduction in the MLP protein level by ∼60% in the myocardium of the patient (Fig. 5D), whereas no changes were observed for other proteins investigated (Fig. 5D). To test whether or not an altered MLP level is a general characteristic of HCM, we analyzed myocardial samples from 17 HCM patients compared with five non-failing control heart samples and found no significant differences (Supplementary Material, Fig. S6).

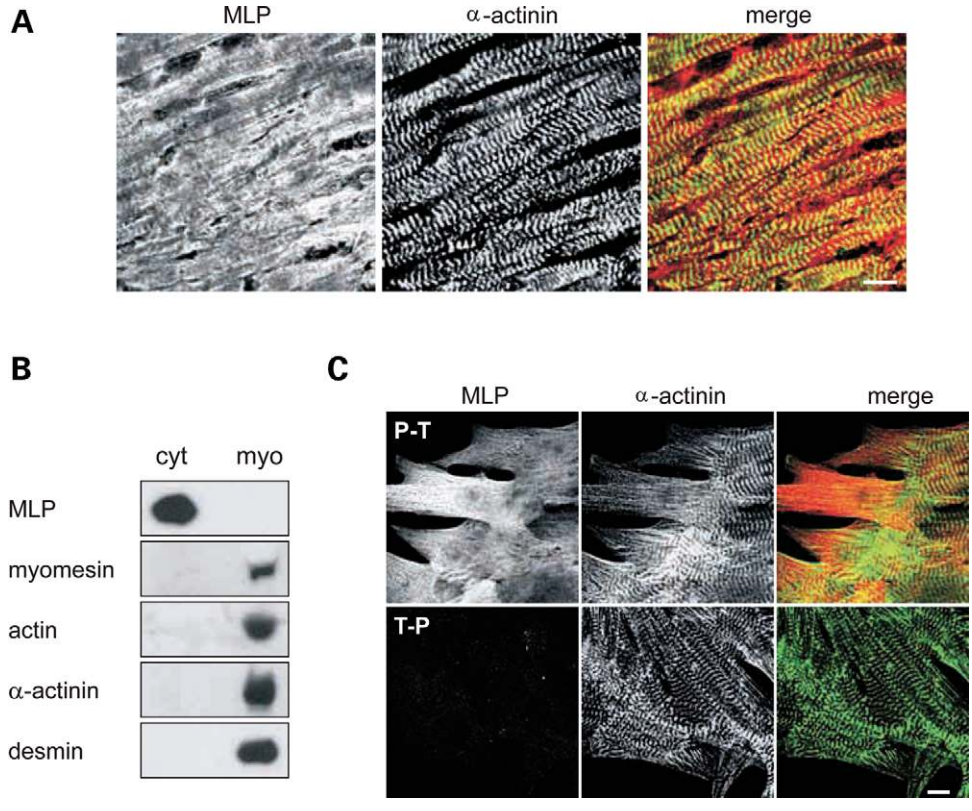

Figure 4. MLP is a cytosolic component of cardiomyocytes. (**A**) Immunofluorescence of MLP in adult mouse myocardium: staining for MLP was diffuse cytoplasmatic. For comparison, Z-discs were visualized by staining for α-actinin; merged picture: MLP, red; α-actinin, green; scale bar is 10 μm. (**B**) Cardiac tissue was fractionated into a cytosolic protein fraction (cyt, soluble protein fraction in low salt Triton X-100 buffer) and an insoluble fraction (myo, containing primarily myofibrillar proteins and also membrane proteins). Equal amounts of both fractions were blotted for the proteins indicated. Note that MLP was extracted quantitatively under the conditions used (lane 1), whereas sarcomeric proteins were not soluble (lane 2), underlining that MLP is primarily a cytoplasmic protein. (**C**) Localization of cytosolic MLP in neonatal cardiomyocytes. First row: cells were fixed and permeabilized according to standard procedures (P–T). Staining for MLP (left) revealed cytoplasmic localization. For comparison, Z-discs were visualized by staining for α-actinin (middle); merged picture: MLP, red; α-actinin, green. When the cells were extracted with Triton X-100 prior to fixation (T–P, second row), staining for MLP was essentially negative, indicating that MLP protein was quantitatively washed out (left). The conservation of sarcomeric structures was demonstrated by staining for α-actinin (middle), merged picture: MLP, red; α-actinin, green; scale bar is 10 μm.

In vitro, the MLP p.C58G mutant protein (14) was less stable in solution than wild-type MLP, and thermolysine digestion resulted in more rapid proteolysis of MLP p.C58G (Fig. 5A and B). The instability of MLP p.C58G was confirmed in transfected COS-1 cells (Fig. 5C). To verify that the relative lack of MLP p.C58G compared with wild-type MLP was not due to the differences at the level of RNA transcription, quantitative reverse transcriptase–polymerase chain reaction (RT–PCR) was performed. COS-1 cells transfected with either wild-type or mutated MLP constructs were used for these analyses. Equal abundance of both mutated and wild-type MLP was observed at RNA level (Supplementary Material, Fig. S7A), confirming that the differences of MLP proteins were due to degradation of the mutated form.

Because MLP is expressed both in myocardium and in slow-twitch skeletal muscle fibers, we searched for skeletal muscle involvement in five HCM patients with *CSRP3* mutations. Three of five patients complained of exertional myalgias and cramps. Two other patients were free of neuromuscular symptoms. In the three symptomatic patients, serum creatine kinase levels were moderately elevated. Histologically, in specimens obtained from the quadriceps or deltoid muscle of two patients, mild myopathic changes were found. A few fibers displayed cytoplasmic accumulation of amorphous material (Fig. 6) that stained positive for desmin and dystrophin (not shown). These findings are considered typical for myofibrillar myopathy (15).

DISCUSSION

We present additional evidence that *CSRP3* is an HCM-causing disease gene (OMIM CMH12, http://www.ncbi.nlm.nih.gov/entrez/dispomim.cgi?id=612124): we found robust linkage to the genomic region of *CSRP3* and identified a heterozygous *CSRP3* missense mutation. The exclusion of all HCM disease genes known to date in this family and the absence of the identified *CSRP3* missense mutations in 1066 chromosomes of control probands, as well as the identification of another four HCM families where disease segregated with the presence of other *CSRP3* mutations, provide further evidence.

Our genetic data suggest that a DCM-associated MLP p.W4R variant (10) (OMIM CMD1M, http://www.ncbi.nlm.nih.gov/entrez/dispomim.cgi?id=607482) may not be sufficient to

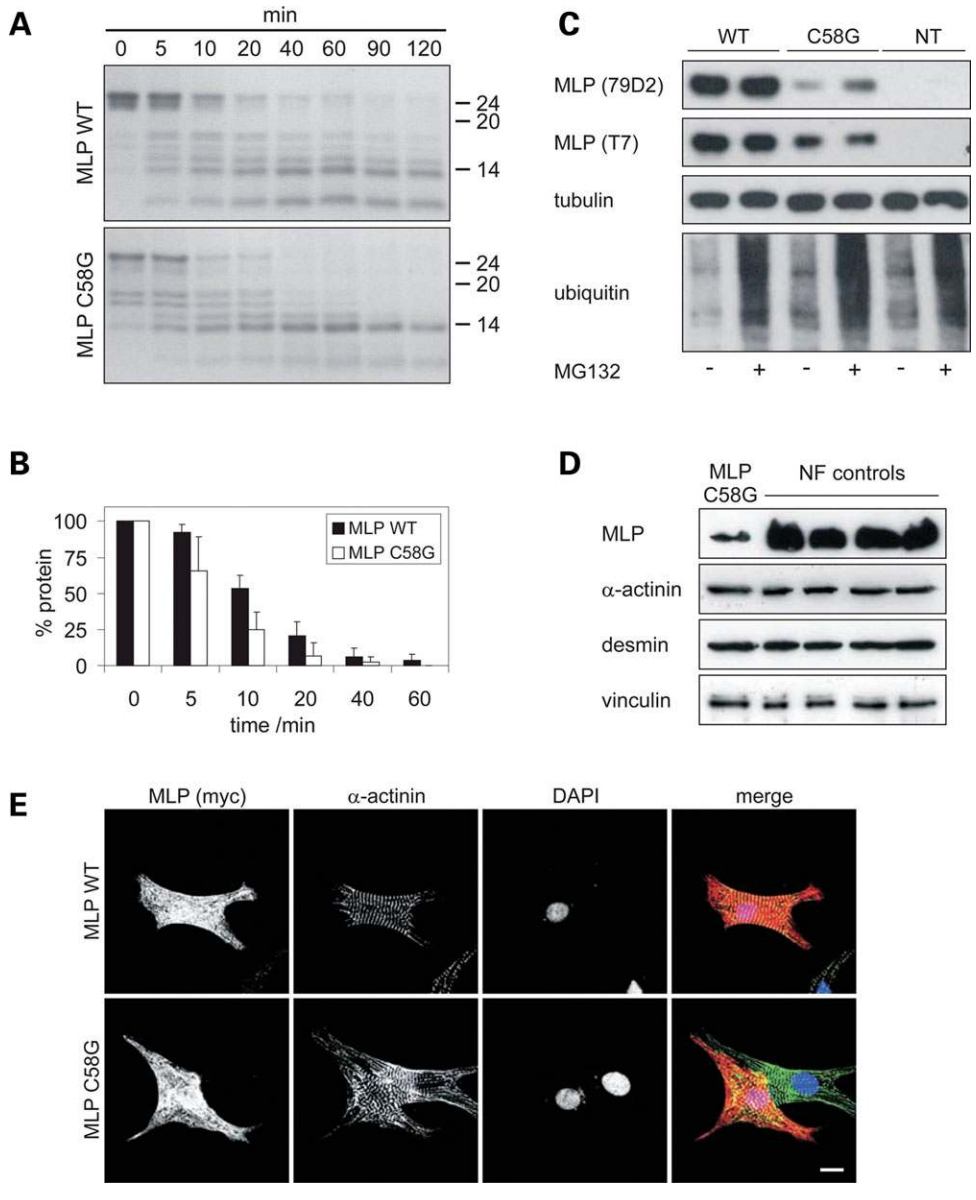

Figure 5. MLP p.C58G protein shows reduced stability *in vitro* and *in vivo*. (**A**) Proteolytic treatment of equal amounts of recombinant purified MLP wild-type (WT) and MLP p.C58G protein resulted in a more rapid and more pronounced degradation of the mutant protein, indicating its reduced stability. The molecular weights of marker proteins are given for comparison. (**B**) Densitometric quantification of un-degraded recombinant wild-type (black bars) and p.C58G MLP (white bars) after different periods of incubation with thermolysine. The quantity of both wild-type and p.C58G MLP before the addition of thermolysine was set at 100%. (**C**) Instability of MLP C58G protein at the cellular level: COS-1 cells were transfected with T7-tagged wild-type MLP construct (WT, 1 μg), T7-tagged mutant MLP p.C58G construct (1 μg) or no DNA (NT). Forty-eight hours after transfection, cells were harvested and total protein extracts were subjected to SDS–PAGE. Blotting with MLP mAB 79D2 and with T7-tag antibody revealed instability of mutant MLP p.C58G protein compared with wild-type MLP. Note that treatment with proteasomal inhibitor MG132 (50 μM for 6 h before harvesting, indicated by '+') did not restore mutant MLP C58G levels to wild-type levels. Blotting for endogenous tubulin served as loading control, the accumulation of poly-ubiquitinated proteins confirmed the inhibition of the proteasome by MG132. (**D**) MLP protein level was found to be dramatically reduced in cardiac biopsies of the MLP p.C58G index patient (III:1 in family H1) when compared with non-failing (NF) human hearts (~40% of wild-type level), whereas protein levels of other proteins were normal. (**E**) Transfection of wild-type and mutant MLP constructs into neonatal rat cardiomyocytes. Cells were transfected using myc-tagged wild-type MLP construct (top row) or MLP construct harbouring the C58G mutation (bottom row). Forty-eight hours after transfection, cells were labeled for myc-tagged constructs (first column), the sarcomeric marker α-actinin (second column) and nuclei were visualized with DAPI (third column). Merged pictures: MLP (myc), red; α-actinin, green; DAPI blue; scale bar is 10 μm. Note that transfected MLP protein is not confined to sarcomeric structures, but rather diffusely distributed throughout cytoplasm and nucleus. No difference was observed between wild-type and mutant MLP protein.

cause cardiomyopathy but could act as a conditional modifier, which would explain the unusually low penetrance in the first report of that mutation. Previous reports of this mutation in unaffected individuals did not role out the possibility that these apparently healthy mutation carriers were in preclinical state of cardiomyopathy nor did other reports of the same mutation in HCM patients examine a cosegregation between the MLP p.W4R variant and HCM (16–18). Our detection of

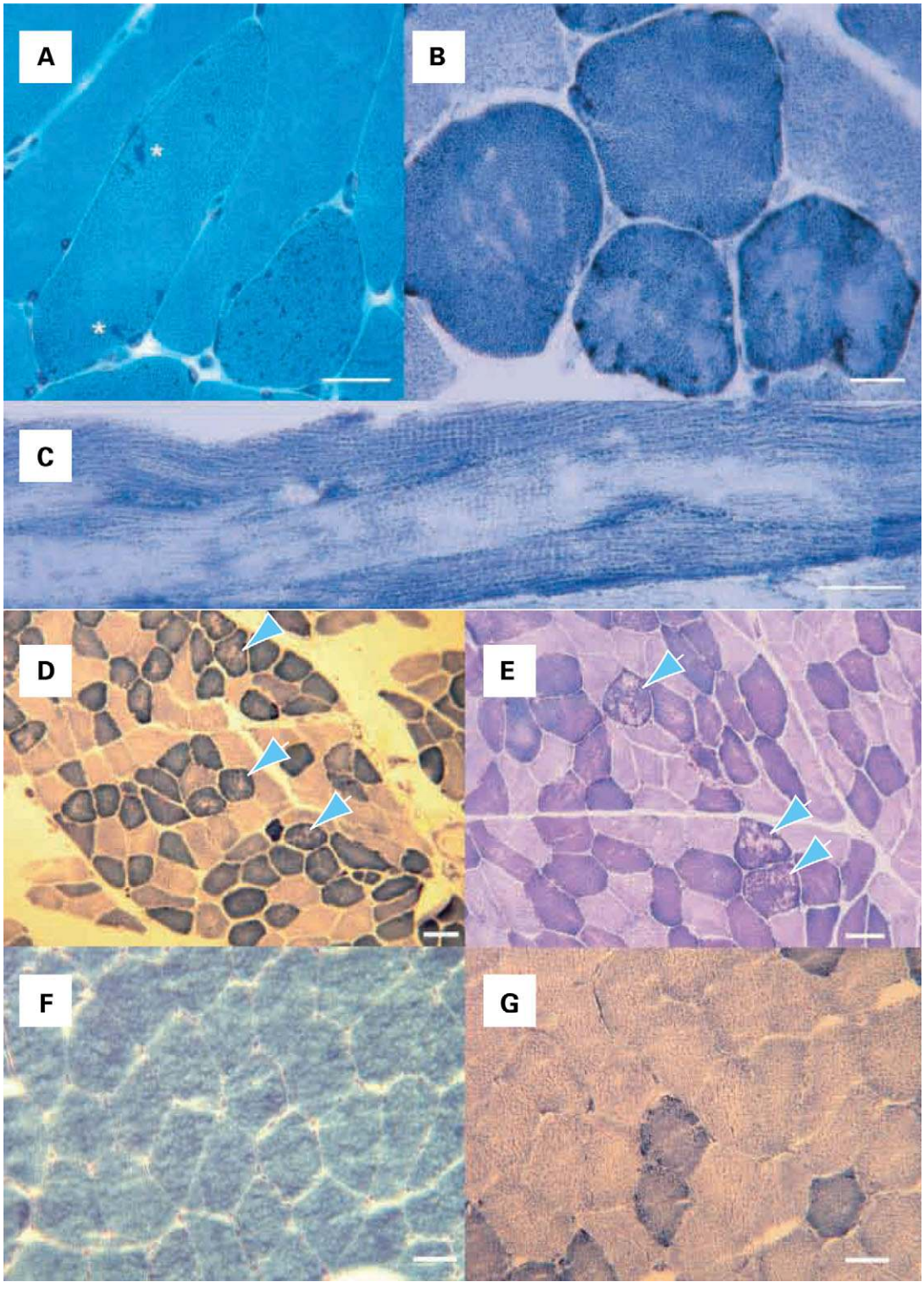

Figure 6. Skeletal muscle in MLP p.C58G (individual III:1 in family H1) demonstrating changes typical of myofibrillar myopathy: (**A**) Gomori-Trichrome stain. Centralized nuclei as well as areas with hyaline amorphous material (asterisks) are found in a small number of fibers. (**B** and **C**) NADH-dehydrogenase stain: areas devoid of enzyme activity in transverse (B) and longitudinal (C) sections. These alterations were not identified in skeletal muscle obtained from an individual with MLP p.W4R (see F and G). (**D**) Low magnification of skeletal muscle in MLP p.C58G demonstrating changes typical of myofibrillar myopathy. As in (A, B and C), skeletal muscle obtained from individual III:1 (Family H1) with MLP p.C58G mutation. NADH-dehydrogenase stain, low magnification. Multiple fibers harbour areas devoid of enzyme activity (arrowheads). (**E**) Similar changes (arrowheads) in NADH-dehydrogenase stain in a muscle specimen obtained from a patient with myofibrillar myopathy due to *DES* c.815 + 1G > A acceptor splice site mutation. (**F, G**). Normal muscle histology in specimen (M. vast. lat.) obtained from individual III:2 (Family D1) with MLP p.W4R (F, Gomori-trichrome stain; G, NADH dehydrogenase). Scale bars represent 80 μm in (D), 60 μm in (E), 40 μm in (F) and (G).

the MLP p.W4R variant in an HCM family, where it does not cosegregate with disease, clearly excludes a causative association of an MLP p.W4R variant and HCM. In that family, a nonsense mutation in the known HCM gene *MYBPC3* could be identified. A similar prevalence (0.4 versus 0.5 versus 0.6%) of the MLP p.W4R variant in large cohorts of both controls and DCM and HCM patients is another strong argument for an innocent polymorphism. We deliberately chose a control group of probands aged $\geq$50 years to eliminate, as far as possible, the uncertainty of age-dependent reduced penetrance. When we applied an age-matched control group (including probands $<$50 years old), we even identified seven control probands (1.3% of the cohort) with the MLP p.W4R variant (data not shown), indicating that this allelic variant might actually be a common polymorphism (19).

As somewhat conflicting results have been previously reported on the localization of MLP within cardiomyocytes, we studied MLP localization with an MLP-specific murine monoclonal antibody. In previous studies based on different polyclonal antisera, localizations were confined either to sarcomeric Z-disk structures, or mainly to the M-band, to costameric sites or even to nuclear location (8,9,20,21). Our results clearly demonstrate that MLP distribution in the myocardium is not confined to sarcomeric structures. This conclusion is supported by fractionation and extraction experiments, showing that MLP is more readily extracted than myofibrillar proteins. Therefore, MLP appears to be a cytosolic protein that might partially be directed to distinct subcellular compartments by various binding partners. Already identified binding partners are α-actinin (22) and telethonin (10) at sarcomeric Z-bands, βI-spectrin (8) at costameres and N-RAP (23) at intercalated disks.

Thus, *CSRP3* represents an HCM disease gene that does not encode a solely sarcomeric protein. The notion that *CSRP3* mutations cause genuine HCM is supported by structural analyses: myocardial biopsies of an HCM patient with a heterozygous *CSRP3* mutation showed all the typical structural abnormalities including myocyte disarray. Myocyte disarray has thus far only been described in HCM patients with sarcomeric protein mutations. Patients with mutations in *LAMP2* or *PRKAG2*, both encoding non-sarcomeric proteins, may clinically present with HCM. However, these patients feature glycogen accumulation within cardiomyocytes in the absence of myocyte disarray or fibrosis (24,25). The term *glycogen cardiomyopathy* has been recommended to name these HCM phenocopy conditions (26).

Compared with wild-type MLP, p.C58G mutant protein was less stable and was more prone to proteolytic decay in solution. These *in vitro* results may reflect reduced stability of mutated MLP protein *in vivo*: first, the mutant protein is also less stable in transfected mammalian cells. Second, the MLP content was dramatically reduced to ~40% in myocardial biopsies in one affected individual harbouring the heterozygous p.C58G MLP mutation. This finding is reminiscent of the reduced MLP levels described as a characteristic of systolic heart failure (27) and is novel for HCM. We therefore tested MLP levels in myocardial samples from HCM patients without *CSRP3* mutations, but found no significant differences to non-failing control heart samples. Since myocardial samples were only available from one patient with *CSRP3* mutation, our finding of reduced MLP content in the absence of congestive heart failure currently only suggests that reduced MLP content is a general phenomenon of HCM-causing *CSRP3* mutations. Analysis of more biopsies is required to confirm this notion. Our preliminary results suggest that the reduction in MLP content in p.C58G MLP myocardium is only partly due to enhanced ubiquitin-dependent proteasomal degradation (Supplementary Material, Fig. S7) and seems, therefore, to differ from the mechanism of *MYBPC3* mutations associated with HCM (28).

From these functional experiments, we reason that not the mutant protein itself but rather the relative lack of functional MLP causes the disease. This interpretation is in line with the phenotype of massive myocardial hypertrophy in a subset of transgenic $MLP^{-/-}$ mice and a mild hypertrophy observed in $MLP^{+/-}$ mice (9).

Interestingly, HCM is associated with mild skeletal myopathy in up to 15% of cases (29). Specific HCM genes may be responsible for this involvement; however, convincing studies testing this hypothesis have not been performed (30). Since MLP is expressed not only in cardiomyocytes but also in slow-twitch skeletal muscle myocytes (31), we also examined patients harbouring *CSRP3* mutations for skeletal muscle abnormalities. Of the five patients available for neuromuscular examination, three patients had a mild myopathy. Our findings in these patients are in line with subtle neuromuscular abnormalities in $MLP^{-/-}$ mice (32). Thus, *CSRP3*–HCM may be the first HCM form convincingly associated with skeletal muscle myopathy. We suggest that all HCM patients undergo careful skeletal muscle testing.

Moreover, our findings on MLP's cellular distribution support the view that the heterogeneous HCM forms are not invariably sarcomeric diseases. Altered sarcomeric function has failed to explain the diverse phenomena observed in HCM, such as enhanced versus impaired myocardial contractility in specific *TNNI* and *MYH7* associated with HCM mutants, respectively (33,34).

Our findings of cytoplasmic MLP localization suggest a review of its proposed mechano-sensory functions (10): it is unlikely that highly soluble MLP, which is not structurally integrated into the cytoskeleton, is directly involved in stress sensing. MLP may rather be understood as a downstream effector, which transduces signals in response to mechanical stress. This notion is in line with the observation that MLP deficiency inhibits the induction of brain natriuretic peptide (BNP) upon mechanical stretch (10). We suggest that defective response to myocardial stress might contribute to the pathogenesis of HCM, or may even be its primary trigger. On basis of heterozygous and homozygous MLP knockout models, we speculate that the impairment of stretch-signalling pathways could be dose dependent: the less is the functional MLP protein, the more impaired the stretch response. In patients, the reduced stability and/or functionality of HCM-associated MLP protein with point mutations may result in impaired response to stretch, leading over decades to inadequate myocyte hypertrophy. This would explain the delayed onset of symptomatic disease in our HCM patients.

Several clues support our hypothesis. Impaired diastolic relaxation as assessed by echocardiographic Doppler tissue imaging is a typical early sign of HCM prior to the onset of

manifest myocardial hypertrophy (35). An altered response to mechanical stress could explain this finding. Another HCM phenomenon that is poorly explained by primary sarcomeric dysfunction is the abnormal hemodynamic adaptation to exercise in some patients (36). Abnormal exercise-induced blood pressure response is a risk factor for sudden cardiac death in HCM patients. This phenomenon could be explained by inadequate signalling in response to mechanical stress. A molecular clue for our hypothesis comes from the recent report that sarcomeric myosin-binding protein C mutations, a major cause of HCM, interacts with MLP (37). Thus, a mutant sarcomeric protein might exert its action via components of the myocardial stress–response pathway. Finally, the typical histological feature of myocyte disarray in HCM could be interpreted as the result of defective stress signalling in the myocardium.

Further research is required to elucidate the molecular basis of stretch-signalling pathways in the heart and the functions of MLP within. We hypothesize that heterozygous $MLP^{+/-}$ mice may develop impaired response to mechanical stress in an age- and/or exercise-dependent manner and, therefore, provide a model system for *CSRP3*-associated HCM. Further studies of these animals should also investigate whether defective calcium cycling (38–40) or energy depletion (41,42) is involved in the pathogenesis of *CSRP3*-associated HCM.

MATERIALS AND METHODS

Clinical evaluation

All clinical and genetic studies were performed according to the Helsinki declaration, and the Charité University Hospital ethical committee approved the studies. Written, informed consent was obtained from all participants. DCM and HCM were diagnosed with established criteria (43,44). An additional major criterion for the diagnosis of HCM based on Doppler echocardiographic parameters of diastolic function (septal $E_a \leq 10$ cm/s in combination with septal $E_a/A_a < 1.0$ and septal $E/E_a > 7$) was applied as suggested previously (11) (note the erroneous value for septal $E/E_a < 7$ instead of > 7 in the cited paper). Physicians unaware of the mutational status of the patients or probands performed all clinical evaluations. Non-failing left ventricular human heart samples were obtained from heart donors whose hearts could not be transplanted for technical reasons. The control group for mutational screening consisted of 533 probands aged ≥ 50 years with documented normal left ventricular size and function and absence of left ventricular hypertrophy.

Genotyping

Genomic DNA was extracted from peripheral blood leukocytes by Puregene kits using an Autopure LS instrument (Qiagen, Hilden, Germany). Singleplex PCR reactions were performed for fluorescence-based semi-automated genotyping. After individual PCR amplification, products were pooled and size fractionated by electrophoresis on ABI 3730 (Applied Biosystems) DNA capillary sequencers. Data were analyzed using *GeneMapper* (v3.0 software, Applied Biosystems).

Linkage, haplotype analysis and mutation detection

Linkage analysis was based on a genome-wide scan using 447 evenly spaced microsatellite markers at an average spacing of 11 cM, from a modified Marshfield Weber 9 Linkage mapping set (Centre for Medical Genetics, Marshfield, WI, USA) covering all 22 autosomes and the X chromosome. An autosomal-dominant model of disease inheritance with reduced penetrance was assumed using a penetrance vector of [0.01; 0.9; 0.9]. Allele frequencies of 0.9999 for the wild-type allele and 0.0001 for the mutant allele were assumed. Two-point LOD score calculations were performed with *MLINK* of the *LINKAGE* v5.2 software package. For haplotyping and computation of multipoint LOD scores, *SIMWALK* v2.83 software was used. Graphical depiction of haplotypes was done with *HaploPainter* software (45). Other pedigrees were painted using *Cyrillic* v2.1.3 software (Cherwell Scientific). Scientists blinded for the mutational status of the individuals did all linkage calculations and haplotype analyses.

We used double-strand sequencing on an ABI 3100 Genetic Analyzer (Applied Biosystems) to search for human *CSRP3* mutations. Of the 652 DCM patients and 354 HCM patients subjected to *CSRP3* sequencing, 400 DCM and 200 HCM patients had previously been screened for CSRP3 mutations (11) with single-strand conformation polymorphism analysis—a less-sensitive method for mutation detection. PCR primers and amplification conditions were as described previously (11). Confirmation of the identified mutations was done by restriction digests of PCR amplicons with restriction enzymes (New England Biolabs): *CSRP3* c.10T>C with *Nci*I and *Bsr*I; *CSRP3* c.131T>C with *Nla*IV; *CSRP3* c.136A>C with *Aci*I; *CSRP3* [c.160T>A; c.161C>G; c.164A>G] with *Bgl*II and *Hin*fI; and *CSRP3* c.172T>G with *Bce*AI.

Histology and immunofluorescence

For electron microscopy, biopsies and mouse myocardial samples were immersion fixed in sodium cacodylate (75 mM, pH 7.5) buffered 2% glutaraldehyde supplemented with 3 mM $MgCl_2$ for 36 h and rinsed in 0.1 M sodium cacodylate (pH 7.5), osmicated with 1% osmium tetroxide in 0.1 M sodium cacodylate buffer for 2 h, dehydrated in ethanol series and embedded in Poly/Bed 812 (Polysciences) according to standard procedures. Semithin sections (1.0 μm) were stained with toluidine blue. Ultrathin sections (70 nm) were contrasted with uranyl acetate and lead citrate and examined with a Philips 400 T electron microscope.

Paraffin-embedded myocardial biopsy sections (10 μm) were stained with either hematoxylin-eosin or Picrosirius red by routine protocols. Serial sections of skeletal muscle biopsies were subjected to standard staining procedures with hematoxylin-eosin, Gomori-Trichrome stain or NADH dehydrogenase.

For immunohistochemistry, myocardial samples were mounted on Gum Tragacanth supported on cork plates and snap frozen in isopentane cooled in liquid nitrogen. In the same way, skeletal muscle biopsies were mounted and snap frozen. Confocal immunofluorescence microscopy of NRCs, skeletal and cardiac muscle sections (6–10 μm) was performed essentially as described previously (46). For extraction

experiments, NRCs (see below) were extracted with 0.2% Triton X-100 in phosphate buffered saline (PBS) for 1 min prior to standard paraformaldehyde fixation and immunofluorescence analysis. 4',6-diamidino-2-phenylindole (DAPI, Sigma) was used to visualize nuclei, F-actin stained with phalloidin conjugated to Alexa Fluor 633 (Molecular Probes). Images were taken from single confocal sections on a Zeiss 510 confocal microscope, equipped with 405 nm blue diode, argon and helium neon lasers using a ×63/1.32 oil immersion lens and processed with Adobe Photoshop.

Antibodies

For the generation of the monoclonal MLP antibody 79D2, NZB mice were immunized with a synthetic peptide identical to 20 amino acids of human MLP C-terminus coupled to keyhole limpet haemocyanin. Standard procedures for the generation of hybridoma cell lines as well as for subcloning and antibody purification were applied. Apart from this MLP mAB 79D2, the following antibodies were used in the study: myomesin polyclonal rabbit serum (pR) WO6 (47), pan-actin pR (Sigma), α-actinin 2 pR 653 (14), vinculin mAB Vin11.5 (Sigma), desmin mAB D33 (Dako), myc mAB antibody (Roche), T7 mAB (Novagen), ubiquitin pR (Dako) and tubulin mAB DM1A (Sigma).

Protein extraction, protein biochemistry and western blotting

For protein fractionation, cardiac tissue samples were snap frozen in liquid nitrogen, ground to powder and resuspended in ice-cold low-salt buffer (1% Triton X-100, 20 mM Tris/HCl, pH 7.6, 138 mM sodium chloride, 5 mM dithiothreitol, protease inhibitors) and incubated on ice for 60 min. Subsequently, the soluble cytosolic protein fraction was clarified by centrifugation at 50 000*g* at 4°C for 15 min. The insoluble fraction, containing myofibrillar and membrane proteins, was washed twice with low-salt buffer. Equal volumes of both fractions were mixed with two times concentrated Laemmli buffer, incubated at 100°C for 3 min and sonicated.

Sodium dodecyl sulfate polyacrylamide gel electrophoresis (SDS-PAGE) and western blotting were performed as described previously (14). For quantification of MLP in myocardial samples, levels of α-actinin were used to normalize MLP contents of the samples, since α-actinin is a myocardial protein whose quantity is identical in both unfailing and failing and hypertrophied cardiomyocytes (48). Densitometric quantification of western blots was performed using Biorad *Quantity One* software. Experiments were repeated twice and one representative data set is shown (expressed as mean ± SEM). Unpaired Student's *t*-tests were performed, and $P < 0.05$ was considered significant.

Recombinant protein expression

For *in vitro* experiments, recombinant CRP1, CRP2, wild-type MLP and mutant (MLP p.C58G) proteins were bacterially expressed and purified as described previously (14). For protein stability assays, equal amounts of wild-type and mutant MLP proteins were treated with thermolysine (Sigma; molar ratio, MLP:thermolysine=3000:1) in PBS at 37°C. After the times indicated, adding Laemmli buffer stopped the reaction. Proteolytic products were resolved by SDS–PAGE using a Tris–Tricine buffer system and visualized with Coomassie. Densitometric quantification was performed as described earlier. For antigen-blocking assays, the mAB 79D2 (50 μg/ml) was incubated with either no protein or wild-type CRP1 (0.5 mg/ml) or wild-type MLP (0.5 mg/ml) in 1% (w/v) bovine serum albumin (BSA) in PBS at 4°C overnight. After centrifugation, these reactions were used in western blotting (diluted 1:50) and immunofluorescence (dilution 1:5) experiments as described earlier.

Cell culture and transfection studies

Isolation and culture of NRCs was performed as described previously (46). Transfection of NRCs was performed as described (46) using wild-type and mutant MLP as myc-tagged constructs (49). Culture and transfection of non-muscle PtK2 and COS-1 cells was performed as described previously using CRP1 and MLP as GFP fusion constructs for PtK2 and T7-tagged constructs for COS-1 cells (46,50). COS-1 cells were treated with the proteasomal inhibitor MG132 (50 μM, Sigma) 6 h before harvesting when indicated.

For transcription studies, COS-1 cells were co-transfected with constructs harbouring T7-tagged human MLP (wild-type versus C58G mutant) and EGFP and were harvested 24 h post-transfection.

Quantitative real-time RT–PCR (TaqMan)

cDNA was synthesized from 5 μg of total RNA isolated from COS-1 cells transiently transfected with MLP–WT or MLP p.C58G constructs, respectively, using PowerScript Reverse Transcriptase (BD Bioscience Clontech) and an Oligo $(dT)_{18}$ primer. Real-time PCR experiments were performed using the Mx3000P® real-time PCR system (Stratagene Europe, Amsterdam, the Netherlands) and the Brillant QPCR master mix (Stratagene Europe).

Real-time PCR was performed for human MLP and with non-pooled samples. *TUBA4*-encoding α-tubulin was used as endogenous reference to normalize expression of a target gene and co-transfected EGFP was used to compare the transfection efficiency.

The following primer/probe sequences were used: for *CSRP3*: F, 5′-GGC CTG CAG TTC CAA CAG T-3′; R, 5′-GGA AGG GTT GCT GGT GGT AA-3′; and FAM-CCC AAA GCC GGC ACG CTC-TAMRA; for *TUBA4*: F, 5′-ACA TTT CCA ACT CTG GAA GCA A-3′; R, 5′-CCA CTC CCA AAC CCT CAT AA-3′; and FAM-CTT GGC CCA GGC TCC TCT GTG C-TAMRA; for *EGFP*: F, 5′-TCC GCC CTG AGC AAA GA-3′; R, 5′-CGA ACT CCA GCA GGA CCA T-3′; and FAM-CCC AAC GAG AAG CGC GAT CA-TAMRA. Annealing temperature was 58°C. The experiments were performed in triplicates.

SUPPLEMENTARY MATERIAL

Supplementary Material is available at HMG Online.

ACKNOWLEDGEMENTS

We are indebted to the families who participated in this study, to Elena Schmidt for technical assistance with genetic analyses, to Ulrik Baandrup for support in electron microscopy and to Friedrich C. Luft for comments and suggestions on the manuscript.

Conflict of Interest statement. None declared.

FUNDING

This study was supported in part by the Max Delbrück Center for Molecular Medicine Berlin-Buch (to C.G.), the German Federal Ministry of Science and Education through the National Genome Research Network (to P.N.) and the German Competence Network Heart Failure (Kompetenznetz Herzinsuffizienz), by the Charité Universitätsmedizin Berlin, and the Berlin Institute of Heart Research (BIHR), a virtual institute funded by the Helmholtz-Gemeinschaft, and the Deutsche Forschungsgemeinschaft (grant KFG192 to S. Spuler).

REFERENCES

1. Maron, B.J., Gardin, J.M., Flack, J.M., Gidding, S.S., Kurosaki, T.T. and Bild, D.E. (1995) Prevalence of hypertrophic cardiomyopathy in a general population of young adults. Echocardiographic analysis of 4111 subjects in the CARDIA study. Coronary Artery Risk Development in (Young) Adults. *Circulation*, **92**, 785–789.
2. Maron, B.J., Olivotto, I., Spirito, P., Casey, S.A., Bellone, P., Gohman, T.E., Graham, K.J., Burton, D.A. and Cecchi, F. (2000) Epidemiology of hypertrophic cardiomyopathy-related death: revisited in a large non-referral-based patient population. *Circulation*, **102**, 858–864.
3. Maron, B.J., Sato, N., Roberts, W.C., Edwards, J.E. and Chandra, R.S. (1979) Quantitative analysis of cardiac muscle cell disorganization in the ventricular septum. Comparison of fetuses and infants with and without congenital heart disease and patients with hypertrophic cardiomyopathy. *Circulation*, **60**, 685–696.
4. Thierfelder, L., Watkins, H., MacRae, C., Lamas, R., McKenna, W., Vosberg, H.P., Seidman, J.G. and Seidman, C.E. (1994) Alpha-tropomyosin and cardiac troponin T mutations cause familial hypertrophic cardiomyopathy: a disease of the sarcomere. *Cell*, **77**, 701–712.
5. Richard, P., Villard, E., Charron, P. and Isnard, R. (2006) The genetic bases of cardiomyopathies. *J. Am. Coll. Cardiol.*, **48**, A79–A89.
6. Van Driest, S.L., Vasile, V.C., Ommen, S.R., Will, M.L., Tajik, A.J., Gersh, B.J. and Ackerman, M.J. (2004) Myosin binding protein C mutations and compound heterozygosity in hypertrophic cardiomyopathy. *J. Am. Coll. Cardiol.*, **44**, 1903–1910.
7. Richard, P., Charron, P., Carrier, L., Ledeuil, C., Cheav, T., Pichereau, C., Benaiche, A., Isnard, R., Dubourg, O., Burban, M. *et al.* (2003) Hypertrophic cardiomyopathy: distribution of disease genes, spectrum of mutations, and implications for a molecular diagnosis strategy. *Circulation*, **107**, 2227–2232.
8. Flick, M.J. and Konieczny, S.F. (2000) The muscle regulatory and structural protein MLP is a cytoskeletal binding partner of βI-spectrin. *J. Cell Sci.*, **113**, 1553–1564.
9. Arber, S., Hunter, J.J., Ross, J., Jr., Hongo, M., Sansig, G., Borg, J., Perriard, J.C., Chien, K.R. and Caroni, P. (1997) MLP-deficient mice exhibit a disruption of cardiac cytoarchitectural organization, dilated cardiomyopathy, and heart failure. *Cell*, **88**, 393–403.
10. Knöll, R., Hoshijima, M., Hoffman, H.M., Person, V., Lorenzen-Schmidt, I., Bang, M.L., Hayashi, T., Shiga, N., Yasukawa, H., Schaper, W. *et al.* (2002) The cardiac mechanical stretch sensor machinery involves a Z disc complex that is defective in a subset of human dilated cardiomyopathy. *Cell*, **111**, 943–955.
11. Geier, C., Perrot, A., Özcelik, C., Binner, P., Counsell, D., Hoffmann, K., Pilz, B., Martiniak, Y., Gehmlich, K., van der Ven, P.F. *et al.* (2003) Mutations in the human muscle LIM protein gene in families with hypertrophic cardiomyopathy. *Circulation*, **107**, 1390–1395.
12. Fung, Y.W., Wang, R.X., Heng, H.H. and Liew, C.C. (1995) Mapping of a human LIM protein (CLP) to human chromosome 11p15.1 by fluorescence in situ hybridization. *Genomics*, **28**, 602–603.
13. Erdmann, J., Raible, J., Maki-Abadi, J., Hummel, M., Hammann, J., Wollnik, B., Frantz, E., Fleck, E., Hetzer, R. and Regitz-Zagrosek, V. (2001) Spectrum of clinical phenotypes and gene variants in cardiac myosin-binding protein C mutation carriers with hypertrophic cardiomyopathy. *J. Am. Coll. Cardiol.*, **38**, 322–330.
14. Gehmlich, K., Geier, C., Osterziel, K.J., Van der Ven, P.F. and Fürst, D.O. (2004) Decreased interactions of mutant muscle LIM protein (MLP) with N-RAP and alpha-actinin and their implication for hypertrophic cardiomyopathy. *Cell Tissue Res.*, **317**, 129–136.
15. Selcen, D., Ohno, K. and Engel, A.G. (2004) Myofibrillar myopathy: clinical, morphological and genetic studies in 63 patients. *Brain*, **127**, 439–451.
16. Mohapatra, B., Jimenez, S., Lin, J.H., Bowles, K.R., Coveler, K.J., Marx, J.G., Chrisco, M.A., Murphy, R.T., Lurie, P.R., Schwartz, R.J. *et al.* (2003) Mutations in the muscle LIM protein and alpha-actinin-2 genes in dilated cardiomyopathy and endocardial fibroelastosis. *Mol. Genet. Metab.*, **80**, 207–215.
17. Bos, J.M., Poley, R.N., Ny, M., Tester, D.J., Xu, X., Vatta, M., Towbin, J.A., Gersh, B.J., Ommen, S.R. and Ackerman, M.J. (2006) Genotype–phenotype relationships involving hypertrophic cardiomyopathy-associated mutations in titin, muscle LIM protein, and telethonin. *Mol. Genet. Metab.*, **88**, 78–85.
18. Newman, B., Cescon, D., Woo, A., Rakowski, H., Erikkson, M.J., Sole, M., Wigle, E.D. and Siminovitch, K.A. (2005) W4R variant in CSRP3 encoding muscle LIM protein in a patient with hypertrophic cardiomyopathy. *Mol. Genet. Metab.*, **84**, 374–375.
19. Hoshijima, M., Knöll, R., Pashmforoush, M. and Chien, K.R. (2006) Reversal of calcium cycling defects in advanced heart failure toward molecular therapy. *J. Am. Coll. Cardiol.*, **48**, A15–A23.
20. Boateng, S.Y., Belin, R.J., Geenen, D.L., Margulies, K.B., deTombe, P.P. and Russell, B. (2006) A47. Decreased levels of non-nuclear muscle LIM protein are associated with cardiac dysfunction and heart failure. *J. Mol. Cell. Cardiol.*, **40**, 864.
21. Kong, Y., Flick, M.J., Kudla, A.J. and Konieczny, S.F. (1997) Muscle LIM protein promotes myogenesis by enhancing the activity of MyoD. *Mol. Cell. Biol.*, **17**, 4750–4760.
22. Louis, H.A., Pino, J.D., Schmeichel, K.L., Pomies, P. and Beckerle, M.C. (1997) Comparison of three members of the cysteine-rich protein family reveals functional conservation and divergent patterns of gene expression. *J. Biol. Chem.*, **272**, 27484–27491.
23. Ehler, E., Horowits, R., Zuppinger, C., Price, R.L., Perriard, E., Leu, M., Caroni, P., Sussman, M., Eppenberger, H.M. and Perriard, J.C. (2001) Alterations at the intercalated disk associated with the absence of muscle Lim protein. *J. Cell Biol.*, **153**, 763–772.
24. Arad, M., Maron, B.J., Gorham, J.M., Johnson, W.H., Jr., Saul, J.P., Perez-Atayde, A.R., Spirito, P., Wright, G.B., Kanter, R.J., Seidman, C.E. *et al.* (2005) Glycogen storage diseases presenting as hypertrophic cardiomyopathy. *N. Engl. J. Med.*, **352**, 362–372.
25. Arad, M., Benson, D.W., Perez-Atayde, A.R., McKenna, W.J., Sparks, E.A., Kanter, R.J., McGarry, K., Seidman, J.G. and Seidman, C.E. (2002) Constitutively active AMP kinase mutations cause glycogen storage disease mimicking hypertrophic cardiomyopathy. *J. Clin. Invest.*, **109**, 357–362.
26. Ahmad, F., Seidman, J.G. and Seidman, C.E. (2005) The genetic basis for cardiac remodeling. *Annu. Rev. Genomics Hum. Genet.*, **6**, 185–216.
27. Zolk, O., Caroni, P. and Böhm, M. (2000) Decreased expression of the cardiac LIM domain protein MLP in chronic human heart failure. *Circulation*, **101**, 2674–2677.
28. Sarikas, A., Carrier, L., Schenke, C., Doll, D., Flavigny, J., Lindenberg, K.S., Eschenhagen, T. and Zolk, O. (2005) Impairment of the ubiquitin-proteasome system by truncated cardiac myosin binding protein C mutants. *Cardiovasc. Res.*, **66**, 33–44.
29. Karandreas, N., Stathis, P., Anastasakis, A., Rigopoulos, A., Piperos, P., Theopistou, A., Stefanadis, C. and Toutouzas, P. (2000) Electromyographic evidence of subclinical myopathy in hypertrophic cardiomyopathy. *Muscle Nerve*, **23**, 1856–1861.
30. Anastasakis, A., Karandreas, N., Stathis, P., Rigopoulos, A., Theopistou, A., Sepp, R., Elliott, P.M., Panagiotakos, D.B., Stefanadis, C. and Toutouzas, P. (2003) Subclinical skeletal muscle abnormalities in patients

with hypertrophic cardiomyopathy and their relation to clinical characteristics. *Int. J. Cardiol.*, **89**, 249–256.
31. Arber, S., Halder, G. and Caroni, P. (1994) Muscle LIM protein, a novel essential regulator of myogenesis, promotes myogenic differentiation. *Cell*, **79**, 221–231.
32. Barash, I.A., Mathew, L., Lahey, M., Greaser, M.L. and Lieber, R.L. (2005) Muscle LIM protein plays both structural and functional roles in skeletal muscle. *Am. J. Physiol. Cell Physiol.*, **289**, C1312–C1320.
33. Elliott, K., Watkins, H. and Redwood, C.S. (2000) Altered regulatory properties of human cardiac troponin I mutants that cause hypertrophic cardiomyopathy. *J. Biol. Chem.*, **275**, 22069–22074.
34. Lowey, S. (2002) Functional consequences of mutations in the myosin heavy chain at sites implicated in familial hypertrophic cardiomyopathy. *Trends Cardiovasc. Med.*, **12**, 348–354.
35. Nagueh, S.F., Bachinski, L.L., Meyer, D., Hill, R., Zoghbi, W.A., Tam, J.W., Quinones, M.A., Roberts, R. and Marian, A.J. (2001) Tissue Doppler imaging consistently detects myocardial abnormalities in patients with hypertrophic cardiomyopathy and provides a novel means for an early diagnosis before and independently of hypertrophy. *Circulation*, **104**, 128–130.
36. Campbell, R., Manyari, D.E., McKenna, W.J. and Frenneaux, M. (2003) What is the mechanism of abnormal blood pressure response on exercise in hypertrophic cardiomyopathy? *J. Am. Coll. Cardiol.*, **41**, 2102. author reply 2102–2104.
37. Knöll, R., Carrier, L., Holm, T., Braach, M., Ross, J., Jr., Schmidt, A., Hasenfuß, G., Kögler, H. and Chien, K.R. (2006) MLP is a pivotal genetic modifier of the cardiomyopathic phenotype during Myosin Binding Protein C deficiency. *Clin. Res. Cardiol.*, **95**, V678.
38. Bonne, G., Carrier, L., Richard, P., Hainque, B. and Schwartz, K. (1998) Familial hypertrophic cardiomyopathy: from mutations to functional defects. *Circ. Res.*, **83**, 580–593.
39. Su, Z., Yao, A., Zubair, I., Sugishita, K., Ritter, M., Li, F., Hunter, J.J., Chien, K.R. and Barry, W.H. (2001) Effects of deletion of muscle LIM protein on myocyte function. *Am. J. Physiol. Heart Circ. Physiol.*, **280**, H2665–H2673.
40. Semsarian, C., Ahmad, I., Giewat, M., Georgakopoulos, D., Schmitt, J.P., McConnell, B.K., Reiken, S., Mende, U., Marks, A.R., Kass, D.A. *et al.* (2002) The L-type calcium channel inhibitor diltiazem prevents cardiomyopathy in a mouse model. *J. Clin. Invest.*, **109**, 1013–1020.
41. Ashrafian, H., Redwood, C., Blair, E. and Watkins, H. (2003) Hypertrophic cardiomyopathy:a paradigm for myocardial energy depletion. *Trends Genet.*, **19**, 263–268.
42. Watkins, H. (2003) Genetic clues to disease pathways in hypertrophic and dilated cardiomyopathies. *Circulation*, **107**, 1344–1346.
43. Mestroni, L., Maisch, B., McKenna, W.J., Schwartz, K., Charron, P., Rocco, C., Tesson, F., Richter, A., Wilke, A. and Komajda, M. (1999) Guidelines for the study of familial dilated cardiomyopathies. Collaborative Research Group of the European Human and Capital Mobility Project on Familial Dilated Cardiomyopathy. *Eur. Heart J.*, **20**, 93–102.
44. McKenna, W.J., Spirito, P., Desnos, M., Dubourg, O. and Komajda, M. (1997) Experience from clinical genetics in hypertrophic cardiomyopathy: proposal for new diagnostic criteria in adult members of affected families. *Heart*, **77**, 130–132.
45. Thiele, H. and Nürnberg, P. (2005) HaploPainter: a tool for drawing pedigrees with complex haplotypes. *Bioinformatics.*, **21**, 1730–1732.
46. Lange, S., Auerbach, D., McLoughlin, P., Perriard, E., Schäfer, B.W., Perriard, J.C. and Ehler, E. (2002) Subcellular targeting of metabolic enzymes to titin in heart muscle may be mediated by DRAL/FHL-2. *J. Cell Sci.*, **115**, 4925–4936.
47. Obermann, W.M., Gautel, M., Steiner, F., van der Ven, P.F., Weber, K. and Fürst, D.O. (1996) The structure of the sarcomeric M band: localization of defined domains of myomesin, M-protein, and the 250-kD carboxy-terminal region of titin by immunoelectron microscopy. *J. Biol. Chem.*, **134**, 1441–1453.
48. Aquila, L.A., McCarthy, P.M., Smedira, N.G., Young, J.B. and Moravec, C.S. (2004) Cytoskeletal structure and recovery in single human cardiac myocytes. *J. Heart Transplant.*, **23**, 954–963.
49. van der Ven, P.F., Ehler, E., Vakeel, P., Eulitz, S., Schenk, J.A., Milting, H., Micheel, B. and Fürst, D.O. (2006) Unusual splicing events result in distinct Xin isoforms that associate differentially with filamin c and Mena/VASP. *Exp. Cell Res.*, **312**, 2154–2167.
50. Gehmlich, K., Pinotsis, N., Hayess, K., van der Ven, P.F., Milting, H., El Banayosy, A., Korfer, R., Wilmanns, M., Ehler, E. and Fürst, D.O. (2007) Paxillin and ponsin interact in nascent costameres of muscle cells. *J. Mol. Biol.*, **369**, 665–682.